Journal of Power Sources 254 (2014) 241–248

Contents lists available at ScienceDirect

Journal of Power Sources

journal homepage: www.elsevier.com/locate/jpowsour

Enhancement in cycle life of metallic lithium electrodes protected with Fp-silanes

Susanna Neuhold [b], John T. Vaughey [a], Christa Grogger [b], Carmen M. López [a,*]

[a] Electrochemical Energy Storage, Chemical Sciences and Engineering Division, Argonne National Laboratory, 9700 South Cass Ave., Argonne, IL 60439-4837, USA
[b] Institute of Inorganic Chemistry, Graz University of Technology, A-8010 Graz, Austria

HIGHLIGHTS

- We developed new protective coatings for metallic lithium electrodes.
- Fp-silanes coating agents with different organic substituents were investigated.
- Galvanostatic cycling and EIS were used to evaluate performance of coated electrodes.
- Enhancement of cycle life of up to 500% of coated vs. uncoated lithium in coin cells.
- Mechanism of protection and coating formation are proposed.

ARTICLE INFO

Article history:
Received 11 September 2013
Received in revised form
26 November 2013
Accepted 6 December 2013
Available online 19 December 2013

Keywords:
Lithium
Battery
Coating
Morphology
Silanes

ABSTRACT

Metallic lithium is a promising anode material whose application in rechargeable batteries has been limited by complicated chemical and morphological changes during cycling. These problems can be addressed by the introduction of protective coatings that help to improve the interphasial properties of these electrodes. In this study we used a dip-coating method to generate protective Fp-silane-derived coatings by direct reaction with the surface of metallic lithium. The effect of these coatings has been investigated by comparing the electrochemical performance of coated vs. uncoated electrodes through galvanostatic cycling and electrochemical impedance spectroscopy (EIS). A cycle life enhancement of up to 500% of that of uncoated lithium was observed. Additionally, we observed a trade-off between the value of the obtained stable capacity and the cycle life, which depended on the type of organic substituent on the silane moiety. These results imply that application-tailored protective coatings might, in the near future, enable the efficient use of metallic lithium electrodes in rechargeable batteries.

1. Introduction

In the first decades of the 21st century, demand for high-performance rechargeable batteries has increased in parallel with the pressing need for renewable energy sources and environmentally-benign transportation technologies. Li-ion batteries, the leading commercially-available battery system, are close to reaching their peak performance in terms of cost, safety and energy density. Therefore, future high-performance batteries will rely on next-generation technologies such as lithium–air, lithium sulfur, lithium metal-based and other, non-lithium systems [1–4]. For lithium-based batteries, metallic lithium anodes are of special interest because they have several advantages when compared to graphitic electrodes currently in use. Metallic lithium has a very negative redox potential (−3.03 V vs. NHE) combined with a very low atomic weight (6.94 g mol^{-1}) and large specific capacity (~3862 mAh g^{-1}) [5,6]. The highest energy density of a battery can be achieved with an active metal anode of low redox potential and a high-voltage cathode which makes lithium metal an ideal anode choice [7]. However, widespread commercialization of rechargeable lithium metal batteries has being hindered by limited cyclability and safety issues inherent to this material. As with many metallic electrodes, lithium is morphologically dynamic, which means that it changes shape as it is stripped and plated during electrochemical cycling (e.g. dendrites, porous and mossy growth, surface bubble clusters, volume changes, etc.). These morphology changes drastically affect cycle life by promoting loss of active lithium to form solid electrolyte interface (SEI) films and creating surfaces that catalyze detrimental side reactions. This, in turn, may

* Corresponding author. Present address: CIC Energigune, Albert Einstein 48, 01510 Miñano, Alava, Spain.
E-mail address: clopez@cicenergigune.com (C.M. López).

0378-7753/$ – see front matter © 2013 Elsevier B.V. All rights reserved.
http://dx.doi.org/10.1016/j.jpowsour.2013.12.057

generate safety hazards such as thermal runaway and battery fires [7–10].

Altering the surface kinetics of metallic lithium, by introducing protective layers and coatings that modify the way it behaves during battery operation, can provide a way to avoid these problems. Protective layers can be divided into two main categories: chemical protection and physical protection. Chemical protection refers to coatings formed by direct chemical reaction with the surface of metallic lithium (e.g. in-situ polymerization, formation of Zintl salts, monolayer formation, etc.) [11–16]. Chemically-formed layers protect mainly by changing the kinetics of SEI formation and aging and, to some extent, avoiding direct contact of lithium with the electrolyte. Inhibition of dendrites can also be accomplished because morphological changes are usually closely tied with surface chemistry and kinetics. Physical protection refers to rigid or semi-rigid layers (e.g. ceramic layers, ex-situ formed polymer coatings, separators, etc.) that are in direct contact with lithium without being chemically-bonded to it [17–20]. They protect the electrode mainly by avoiding detrimental side reactions through lack of direct contact with the electrolyte, and by spatially constricting the growth of dendrites. Promising work in water-stable metallic lithium electrodes coated with ceramic membranes has also been reported [21,22]. Additionally, all solid-state battery configurations have been demonstrated to improve the behavior of metallic Li in the lithium–oxygen environment [23,24]. However, the varied conditions under which batteries for different applications operate still require the development of new protective coatings adapted to such electrochemical environments.

Wet-chemistry processing of protective layers is a particularly attractive method due to its ease, scalability, and economy. Additionally, the wide range of chemical reactions available allows for the rational design of coatings with desirable physical, chemical, and electrochemical properties. Among these, organosilane coatings are increasingly used as anti-corrosion pre-treatments on the finishing of metals [25]. More interestingly, silane-based coatings have shown promising performance in the protection of metallic lithium electrodes [12,13,16]. In order to introduce more functionality and introduce more spectroscopic handles, we have investigated the use of alternative silane materials. Cyclopentadienyldicarbonyl iron (II) silanes (Fp-silanes) exhibit reactivity driven by the strong Lewis basicity and nucleophilicity of the Fp-metallate anion. These iron–silicon compounds can be used as precursors for silicon carbides, semiconductors, heat resistant materials, and optical fibers [26,27]. In contact with metallic Li, formation of the Fp-metallate can drive functionalization of the metal surface with the silane moiety, generating a protective, chemically-bound surface coating.

In this study we evaluated the effect on cycle life of metallic lithium electrodes coated with three different Fp-silanes, constructed using a dip-coating, wet-chemistry method. The electrochemical performance of the coated electrodes was evaluated via galvanostatic cycling and electrochemical impedance spectroscopy (EIS). We demonstrate a cyclability enhancement of more than 500% of that of uncoated lithium electrodes in coin cells. Possible mechanism for coating formation and the nature of the protective layers are proposed based on the electrochemical response before and after cycling, the surface morphology of coated vs. uncoated electrodes, and the previously reported reactivity of Fp-silanes.

2. Experimental

2.1. Synthesis of Fp-silanes

Cyclopentadienydicarbonyl iron (II) silanes (Fp-silanes) were synthesized by the electrolysis method described previously [28]. To summarize, an undivided electrolysis cell with a cylindrical stainless steel cathode and a sacrificial magnesium rod anode was used. Both cathode and anode had copper wire contacts, and were etched with diluted nitric acid, polished with sand paper, and dried with compressed air before use. The electrolytic solution was prepared in two steps by (a) preparing a supporting salt solution of 0.02 M tetrabutyl ammonium solution in THF, and (b) adding the appropriate amount of both Fp_2 and chlorosilanes to this solution, followed by 45 min to 2 h of activation on an ultrasonic bath. The amount of Fp_2 and chlorosilanes ($ClSiR_3$), respectively, was: for $FpSiMe_2H$: 9.3 mmol and19.8 mmol, for $FpSiMe_3$: 9.1 mmol and 21.3 mmol, for $FpSiPh_3$: 5.14 mmol and 10.0 mmol. The electrolysis was carried out under galvanostatic mode at average current densities of 15 mA cm^{-2}, until the electrolysis was complete ($\sim$3–14 h). After the electrolysis was finished, the solvent was removed from the product solution under reduced pressure to a volume of approximately 5 mL. 50 mL of dry pentane and 30 mL of dry toluene were added and the solution was filtered over Celite, followed by column chromatographic separation (10 $\times$ 50 cm, silica gel, toluene) under nitrogen.

2.2. Preparation of protective coatings

The lithium anodes were coated with the different Fp-silanes prepared as described above. For the coating process, metallic lithium electrodes were punched from as-received lithium foil (diameter 1.6 cm), without any further cleaning, and dipped into a solution containing one of the different Fp-silanes on EMC. The solution had the same concentration (0.0127 g mL^{-1}) for all compounds used. Electrodes were dipped in the solution for 1, 5, 10, 15 and 30 min, gently rinsed with a few drops of EMC, and allowed to dry in the glove box for 24 h before assembling them into coin cells. The morphology of the coated and uncoated lithium samples was investigated using a Scanning Electron Microscope (FEI Quanta 400 Environmental Scanning Electron Microscope) with a Schottky Field Emission Gun operating at 12.5 kV in high vacuum mode. The lithium samples were prepared in an argon atmosphere glove box (O_2 and H_2O levels $<$ 2 ppm) and transported to the SEM inside a vacuum desiccator. Transfer from the desiccator into the SEM chamber was accomplished in $\sim$10–15 s, which produced no changes in morphology of the surface.

2.3. Electrochemical measurements

Coin cells (Hohsen 2032 cell hardware) were prepared using metallic lithium (FMC Lithium) as anode, $Li_4Ti_5O_{12}$ (LTO) on a copper foil current collector as cathode, a Celgard 2325 separator, and 1.2 M $LiPF_6$/ethylene carbonate (EC):ethyl methyl carbonate (EMC) (30:70 wt%) as the electrolyte (UBE Corporation). The $Li_4Ti_5O_{12}$ electrode was prepared by laminating a mixture of 80 wt% $Li_4Ti_5O_{12}$ (Kyocera), 10 wt% polyvinylidene difluoride in *N*-methyl-2-pyrrolidone binder (Kureha America, Inc.) and 10 wt% acetylene black (Chevron), and drying overnight in a vacuum oven at 70 °C. The thickness of the $Li_4Ti_5O_{12}$ laminate was 0.2 mm as determined by using a stainless steel poc-kit with 5 inches gage assortment (Precision Brand Products, Inc). EIS spectra of the coin cells were recorded using an EG&G model 273A potentiostat and a Solartron model SI1260 frequency response analyzer controlled by ZPLOT (Scribner Associates, Inc.) measurement software. The spectra were recorded in potentiostatic mode in the 10 kHz–50 mHz frequency range with a 10 mV perturbation about the open circuit potential ($\sim$1.56 V vs. Li/Li^+ at 10% state of charge). EIS spectra were recorded as a function of coating time (1, 5, 10, 15 and 30 min), aging time at room temperature (1 h, 2 h, 24 h, 48 h, and 168 h), and after three hundred cycles. The cells were cycled galvanostatically between 1

and 2 V vs. Li/Li^+ (MACCOR Cycler, Series 4000 with MACCOR, Inc. software, version MR 32-bit 2.7.121), at a current density of 2.5 mA cm^{-2}.

3. Results and discussion

The cycle life performance of lithium half cells can be directly correlated with interphasial changes in the metallic lithium electrode under certain conditions. Of key importance is the use of a counter electrode with high stability under the chosen cycling conditions, e.g. LTO, where changes in the cell's performance can be more easily attributed to the lithium anode rather than other issues of construction or testing [8]. In this type of systems, the onset of lithium electrode failure can be pinpointed in the capacity vs. cycle graphs, at the cycle number where an abrupt change in the slope of the graph occurs (Fig. 1a). For metallic Li electrodes treated with three different Fp-substituted silanes, the cycle life performance increased from approximately 60 cycles (unprotected lithium electrodes, Fig. 1a-iv) to 260 cycles (protected with coatings derived from $FpSiPh_3$, (Fig. 1a-i)), or ~430% increase in cycle life. The average capacity per unit area for the unprotected electrodes is 0.63 mAh cm^{-2} and for the best-performing protected electrodes (the $FpSiPh_3$ protected lithium) is 0.59 mAh cm^{-2}, 94% average capacity when compared to the uncoated lithium. The other two Fp-silane derived coatings also increase the cycle life of Li to varying degrees. Electrodes with coatings derived from $FpSiMe_3$ (Fig. 1a-ii) have average cycle life of approximately 130 cycles, and those derived from $FpSiMe_2H$ (Fig. 1a-iii) of more than 300 cycles, or an increase in cycle life of 215%, and more than 500%, respectively. However, increases in cycle life performance are countered by increasing interphasial impedance (Fig. 1b) and lower average capacity in the methyl-substituted coatings than in the phenyl substituted one. Electrodes with coatings derived from $FpSiMe_3$ (Fig. 1a-ii) have average capacities of approximately 0.48 mAh cm^{-2}, and those derived from $FpSiMe_2H$ (Fig. 1a-iii) of 0.26 mAh cm^{-2}, or 76% and 40% average capacity, respectively. The comparative cycle life and stable capacities for the protected and unprotected electrodes are summarized in Table 1. For all the coatings, the diminished capacity appears to be due to an increase in interfacial resistance of the coated electrodes when compared to the uncoated ones (Fig. 1b), probably reflecting thicker coatings that are less permeable to lithium ions.

The cycle life and capacity retention of the coated electrodes was also affected by the time the metallic Li electrodes spend soaking in the Fp-silane/EMC solution. A dip-coating time of 10 min was found to be optimal for $FpSiPh_3$-derived coatings (Figs. 1b-i and 2). For shorter dip-coating times, e.g. 5 min (Fig. 2a-ii), the average cycle life increases to about 144 cycles, with an average stable capacity of 0.67 mAh cm^{-2}, a significant increase in both cycle life and capacity when compared to the uncoated electrode, but not as good as the 10 min dip-coating. At 15 min (Fig. 2b-iv) and 30 min (Fig. 2b-v) dipping times, significant enhancement in cycle life (115, and 255 cycles, respectively) is observed, with acceptable stable capacity (87% and 76%, respectively). However, interphasial impedance steadily rises with coating time (Fig. 2c and d). Additionally, for dip-coating times of 10–30 min, an additional mid-frequency arc can be observed and changes in f_{min} which indicates changes in mass transport in the cell. Furthermore, examination of the impedance spectra of cells with lithium protected with $FpSiPh_3$ at different coating times, and after 300 hundred cycles (Fig. 3a and b) demonstrates the enhanced protection of the 10-min coating. The features of all the spectra are very similar except for three characteristic distinctions: a more pronounced increase in the general impedance of the cell (R_s) for all cells but lower for the $FpSiPh_3$-10 min coating (Fig. 3a-i), changes in f_{min} for all cells, and the number of arcs in the spectra. The general impedance of the cell (R_s), which can be identified from the point at which the highest frequency arc intercepts the real axis, is the sum of the resistances of components of the cell such as electrolyte, current collector, separators, etc. In a previous work, we demonstrated a nearly linear relationship between R_s increase and electrolyte consumption in coin cells containing metallic lithium electrodes [9]. The smaller R_s value for $FpSiPh_3$-10 min coating is compatible with inhibition of electrolyte consumption. In contrast, higher coating times showed higher R_s than either the uncoated or the 10 min-dipped samples (Fig. 3b). f_{min} can be identified from the point where the lowest frequency arc intercepts the diffusion tail and can provide a demarcation between mass-transport controlled processes and interphasial processes [29,30]. The changes observed in f_{min} can therefore be strong indicatives of differences in mass transport within the cell. $FpSiPh_3$-10 min coating shows two arcs in the EIS spectrum similar to uncoated metallic lithium (Fig. 3a-ii and a-iii, respectively), with somewhat less intense arcs for the coated

Table 1
Cycle life performance and stable capacity of coated vs. uncoated lithium electrodes as a function of coating agent.

Coating agent	Avg. cycle life (number of cycles)	% Cycle life vs. uncoated Li	Avg. capacity (mAh cm^{-2})	% Capacity vs. uncoated Li
None	60	–	0.63	–
$FpSiPh_3$	260	430	0.59	94
$FpSiMe_3$	130	215	0.48	76
$FpSiMe_2H$	≥300	500	0.26	40

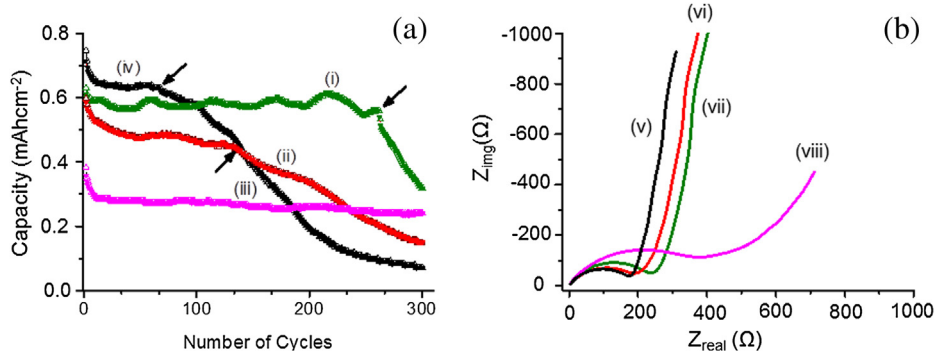

Fig. 1. Effect of coating agent on the electrochemical performance of LTO/coated-lithium cells. (a) Cycling performance of cells; Li electrodes protected with coatings derived from: (i) $FpSiPh_3$, (ii) $FpSiMe_3$, (iii) $FpSiMe_2H$, and that of (iv) uncoated metallic lithium. (b) Impedance spectra of the cells before cycling (2 h room temperature aging): (v) uncoated metallic lithium, (vi) $FpSiMe_3$, (vii) $FpSiPh_3$, (viii) $FpSiMe_2H$.

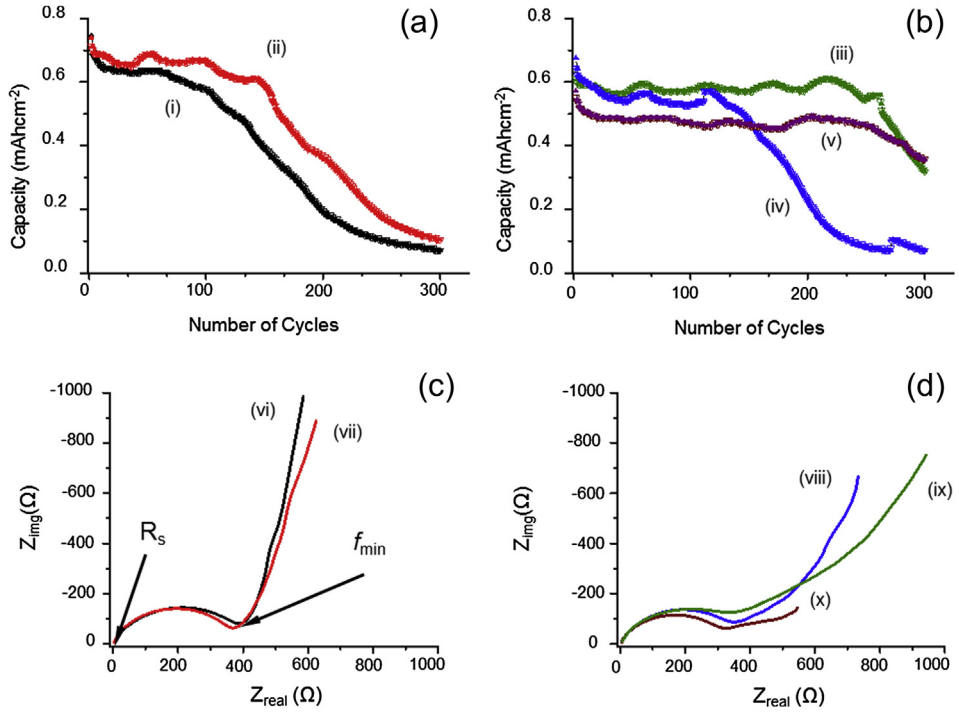

Fig. 2. Effect of dip-coating time on the electrochemical performance of LTO/coated-lithium cells. (a) Cycling performance of electrodes protected with coatings derived from $FpSiPh_3$ at dipping times of: (i) uncoated, (ii) 5 min, (b) (iii) 10 min, (iv) 15 min, and (v) 30 min. Impedance spectra of the cells before cycling, dipping times: (c) (vi) uncoated, (vii) 5 min, (d) (viii) 10 min, (ix) 15 min, and (x) 30 min.

electrode. Longer dip-coating times show only one distinct mid-frequency arc and a mass transport tail. The best trade-off between enhanced cycle life and stable capacity is obtained for the $FpSiPh_3$-derived coating at 10 min dip-coating time. Table 2 summarizes the comparative cycle life and stable capacities for the $FpSiPh_3$-protected electrodes at different dip-coating times. Galvanostatic curves for the uncoated and the $FpSiPh_3$-coated lithium (Fig. 4a and b, respectively) show similar plateaus, dominated by the Li insertion and extraction from the LTO electrode, which rules-out any unusual electrochemical activity of the coating in the cycle life enhancement. It is worth noticing that the electrochemical activity of the Ferrocene moiety lies outside of the potential window of this experiments and could not be evaluated from these results. The difference in cell voltage between the cells containing uncoated lithium and coated lithium can be accounted as a consequence of both cycling rate and interphasial phenomena. Cycling at relatively high cycling rates for this type of electrodes induces an overpotential-related polarization reflected in the voltage hysteresis of the charge–discharge process, as seen in the galvanostatic curves in Fig. 4. The voltage hysteresis in the cells with coated Li (Fig. 4b) is ~140 mV, and in the uncoated lithium (Fig. 4a) ~160 mV. Most of this overpotential is related to mass transport, mainly in the electrolyte, and appears to be related to improved conductivity in the cell with the coated electrodes. Favorable soluble products generated during the first few cycles, during the transformation of the primary SEI into secondary SEI, can be origin of this improvement. This can also be inferred from

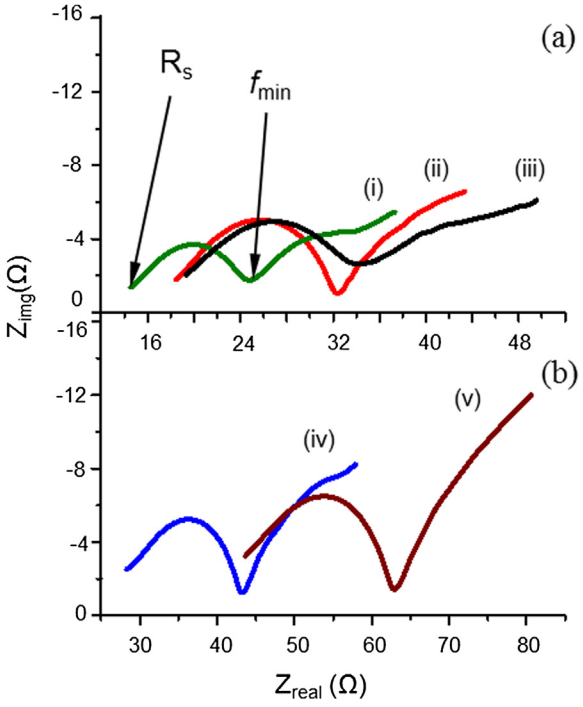

Fig. 3. Effect of dip-coating time on the electrochemical performance of LTO/coated-lithium cells. EIS spectra of the $FpSiPh_3$ coated lithium after cycling for 300 cycles: (a-i) 10 min, (a-ii) 5 min, (a-iii) uncoated, (b-iv) 15 min, and (b-v) 30 min.

Table 2
Cycle life performance and stable capacity of $FpSiPh_3$-coated vs. uncoated lithium electrodes as a function of dip-coating time.

Dip-coating time (min)	Avg. cycle life (number of cycles)	% Cycle life vs. uncoated Li	Avg. capacity (mAh cm^{-2})	% Capacity vs. uncoated Li
0	60	–	0.63	–
5	144	240	0.67	106
10	260	430	0.59	94
15	115	190	0.55	87
30	255	425	0.48	76

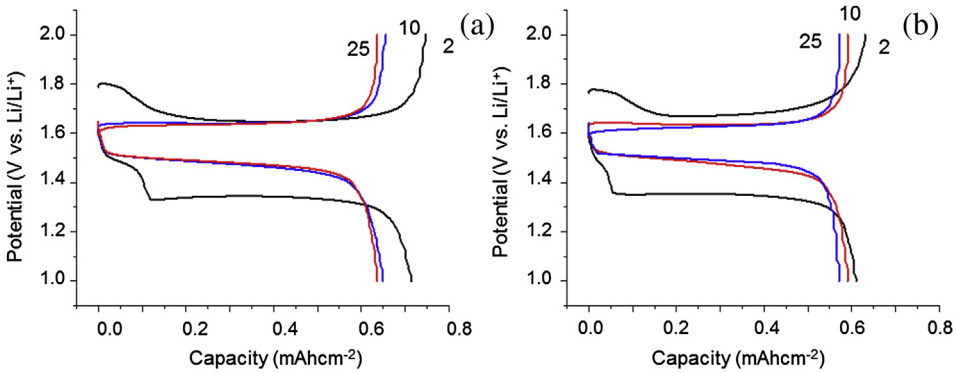

Fig. 4. Electrochemical behavior of uncoated and coated lithium electrodes. Galvanostatic curves obtained at 2 C rate at a number of cycles of 2, 10, and 25, for: (a) uncoated lithium and (b) lithium coated with $FpSiPh_3$.

irreversible capacity during the first 8–10 cycles (Fig. 1a) for all cells, and the difference in the galvanostatic curves from cycles 2, 10, and 25 (Fig. 4). The fact that the voltage hysteresis persists but the galvanostatic curves stabilize after a few cycles supports this hypothesis.

Chemical composition and thickness of the coatings affect the different cycle life enhancements fort the Fp-silane coated lithium. The molecular structure of the different coating agents is shown in Fig. 5. Based on these structures and previous findings, we propose a coating mechanism that involves breaking the Fe–Si bond, with the Fp moiety acting as a leaving agent and resulting in a SiR_3-terminated surface bonded through the surface oxygen group. The known reactivity of other alkyl-silanes towards native specii on the metallic lithium's surface suggests that our chemical coating might proceed by a similar reaction mechanism [12,13]. This is also supported by the surface morphology of the coated electrodes (Fig. 6). The surface morphology of the uncoated and coated electrodes appears almost identical in the low magnification SEM images shown in Fig. 6 (Fig. 6, left column, a, c, e, and g). However, at higher magnifications, textural changes due to coating and identity of coating agents can be clearly observed (Fig. 6, right column, b, d, f, and g). The uncoated lithium electrode without any cleaning or treatment appears "flaky" (Fig. 6b). For the coated electrodes, the ones coated with $FpSiMe_2H$ appears more like a mechanically spread film (Fig. 6d), whereas, $FpSiM_3$ (Fig. 6f), and $FpSiPh_3$ (Fig. 6h) appear less thick and with more particle inclusions.

An important factor for the failure mechanisms of metallic lithium electrodes, the formation and aging of the redox-formed SEI upon first contact with the electrolyte (i.e. primary SEI), has been shown to have a systematic relationship with different failure morphologies for these electrodes [9]. Aging could be electrochemical (originated while cycling the cell), or redox-chemistry (may occur while the battery is in storage or at open circuit potentials). We have recorded the impedance of half cells containing coated and uncoated lithium electrodes during room-temperature storage in order to try to identify the nature of the protective effect. The protective coating derived from the $FpSiPh_3$ agent may have a protective mechanism with strongest effect in redox-chemistry related aging, electrochemistry-related aging, or a combination of both. The EIS spectra in Fig. 7 shows the redox-chemistry related aging for uncoated (Fig. 7a), and $FpSiPh_3$-coated (Fig. 7b) lithium electrodes. From the first high-frequency arc it can be seen that interphasial charge transfer resistance (R_{ct}) increased during aging for both uncoated and coated lithium (Fig. 7a and b, respectively). However, for the $FpSiPh_3$ coated electrode, R_{ct} increase is less than for the uncoated electrode. On the uncoated electrode, the signals of the EIS spectra only show changes in R_{ct} while the Warburg impedance remains unchanged with aging. For the coated electrode, R_{ct} is every time slightly smaller than for the uncoated electrode. The most appreciable difference however, appears in the shape of the Warburg tail. The presence of SEI-type and other thick films can give rise to low-frequency signals that appear linear but do not have the characteristic 45° angle of a purely diffusive or Warburg impedance [9]. The changes in the mass-transport related signals are indicative of possible dissolution of the coating or significant chemical changes due to reaction with the electrolyte. In the freshly prepared cells (Fig. 1b), the charge transfer resistance of unprotected lithium is smaller than that of the cells with any of the coatings. This can be attributed to the nature of the primary SEI formed upon first

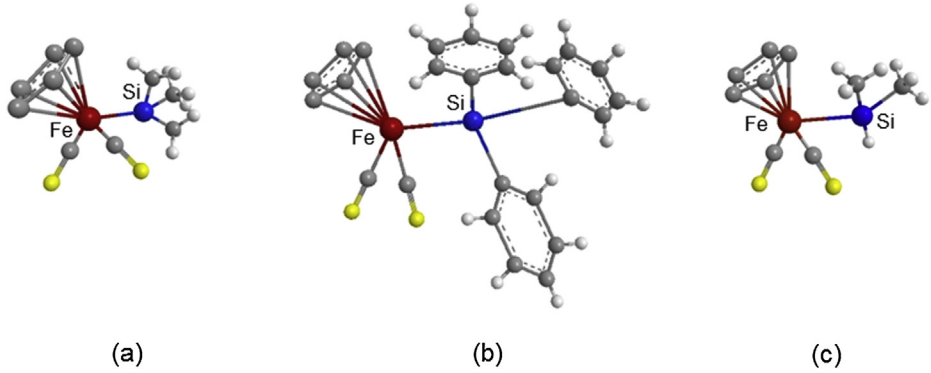

Fig. 5. Chemical structures (ball and stick model) of different Fp-silanes coating agents: (a) $FpSiMe_3$, (b) $FpSiPh_3$, (c) $FpSiMe_2H$. The Fe atoms are indicated in red, Si atoms blue, O yellow, C gray, and H white. (For interpretation of the references to color in this figure legend, the reader is referred to the web version of this article.)

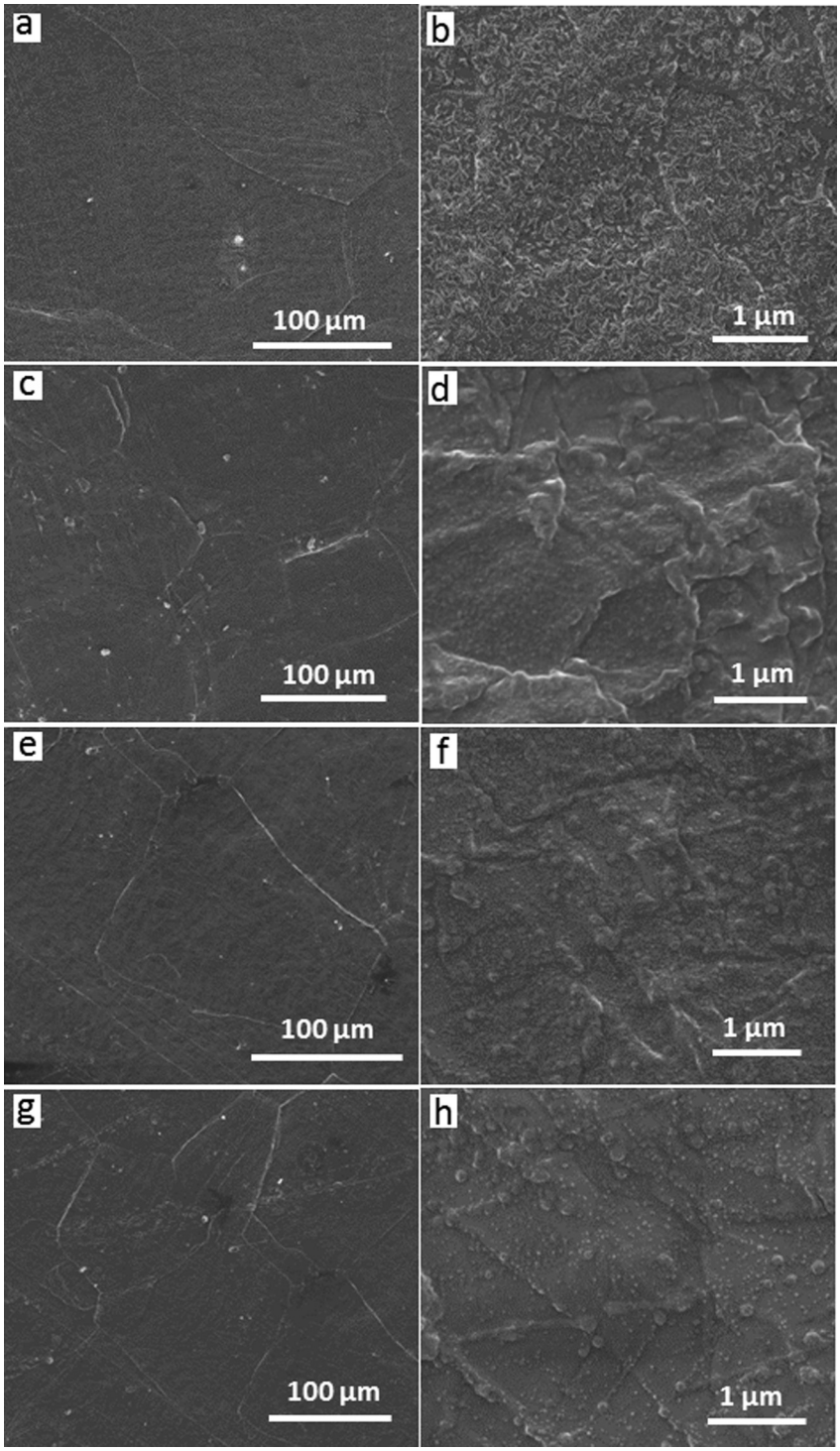

Fig. 6. Surface morphology of coated and uncoated lithium electrodes. SEM images of (a, b) bare metallic lithium, and metallic lithium coated for 10 min with (c, d) $FpSiMe_2H$, (e, f) $FpSiMe_3$, and (g, h) $FpSiPh_3$.

contact with the electrolyte and to the evolution of the secondary SEI during cycling. The primary SEI initially formed in the uncoated electrodes is more conductive than in the coated ones (Fig. 1b), but as it ages it becomes slightly less conductive (Fig. 7). Due to lack of direct contact with the electrolyte, formation and aging of the primary SEI in the coated electrodes is significantly slower than in the uncoated ones (Fig. 7). Additionally, the secondary SEI formed during aging and cycling seems is more conductive in some of the coated electrodes depending on dip-coating time, and the type of substituent in the silane moiety (Figs. 1a, 3, and 7). Primary SEI formation is a continuous process that will occur as long as fresh lithium is exposed to the electrolyte. It competes with secondary SEI formation during cycling and aging, and has a strong effect on the cycling life of cells containing metallic lithium. Indeed, a slightly higher R_{ct} might be an advantage because deleterious redox and electrochemical side reactions that generate inactive lithium can be

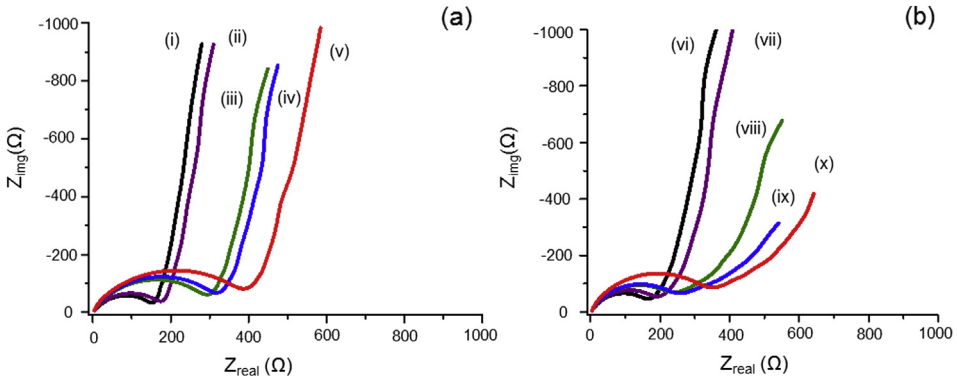

Fig. 7. Evolution of the primary SEI for uncoated and coated lithium electrodes after room temperature aging. Impedance spectra of LTO/lithium cells: (a) uncoated lithium at aging times of (a-i) 10 min, (a-ii) 2 h, (a-iii) 24 h, (a-iv) 48 h, and (a-v) 1 week. (b) lithium coated for 10 min with $FpSiPh_3$ at aging times of (b-vi) 10 min, (b-vii) 2 h, (b-viii) 24 h, (b-ix) 48 h, and (b-x) 1 week.

slowed down due to the slower interphasial kinetics hence, the better cycle life.

Several different aspects of the coating seem to be influencing the cycle life enhancement of the Fp-silane coated lithium electrodes. When comparing different coating agents (Fig. 1) it is clearly seen than the enhanced cycle life is directly proportional to a concomitant decrease in the value of the stable capacity (Fig. 1a), and an increase in R_{ct} of the coated electrodes prior to cycling (Fig. 1b). Therefore, the nature of the protection is possibly tied to avoiding direct contact of the reactive lithium surface with the cell's electrolytes, but also, with the slower kinetics of the interphasial processes. These slower kinetics, in turn, slow down consumption of active lithium and electrolyte, and inhibit dendritic and other forms of detrimental morphology changes. It should be noticed though, that there is a trade-off for this mechanism of lithium protection, (i.e. the longer the cycle life the lower the capacity, Fig. 1a and Table 1), which can nonetheless be tuned to maximize the desirable performance. This can be advantageous for specific applications when tailoring electrodes for longer cycle life and slower cycling.

So far we have identified a clear and systematic dependency between the cycling performance, EIS response, and coating parameters such as molecular structure of the coating agent and dip-coating time. Furthermore, we have utilized EIS of room-temperature aged cells to gain insights into primary SEI evolution during aging of the cell. From the data available we can also obtain some information about the possible chemical mechanisms of the coating process itself. Surface coatings on metallic lithium by reaction with alkyl-substituted chlorosilanes had been found to be self-terminating [11–13]. However, it is not clear yet whether the reaction with the Fp-substituted silanes also works by the same mechanism. The dependence of cycle performance and cell's impedance on dip-coating time shown in Fig. 2, has at least three possible chemistry-related origins. The first possibility is that the reaction proceeds from a slightly different mechanism than other alkyl-substituted silanes, in which case it might form significantly thicker coatings before the reaction is inhibited and the lithium surface becomes effectively passivated. Second, the coating reaction could be indeed self-terminating reaction. In this case it is possible that after the growth of a few monolayers of coating, the reaction does not proceed anymore and the unreacted precursor just physically sticks to the surface producing higher impedance and then dissolving in the electrolyte when the cell is assembled. The third possibility is an extension of the second, but assuming no significant unreacted residue remains. In this case the reaction is self-terminating but the degree of coverage and therefore the thickness of the coating depend on the size and nature of the alkyl substituent. By extension, the bulkiness of the substituents and whether they can form more conductive or insulating layers (methyl groups vs. phenyl groups) can also be an important parameter. It can be seen from Fig. 6 (surface morphology) and Fig. 1 (EIS vs. coating agent) that the rugosity of the coated lithium has a correlation with R_{ct} and with the bulkiness and number of alkyl substituents on the Si atom. $SiPh_3$ appears to form the thinner-looking coatings, although it exhibits a slightly higher R_{ct} than $SiMe_3$, possibly due to the difference in aging between the two coatings. (Cycling performance and the EIS spectra shown in Figs. 1 and 3 are recorded in cells aged for 1 week at room temperature.) The impedance spectra recorded after 300 cycles offers some clues to the stability of the $FpSiPh_3$-derived coatings, but is does not really clarify if coating reaction is self-terminating or not. The longer dipping times are not necessarily the ones showing lower impedance after cycling, neither in R_{ct} nor in R_s. One would expect that the longer dip-coating times would produce thicker coatings and therefore less contact with the electrolyte. Thicker coatings however, may prevent an effective washing of Fp-residues which might then react with the electrolyte inside the cell, producing more resistive and/or less stable coatings (Fig. 3). Therefore, optimization of coating thickness by choosing different substituents on the silane group can provide an avenue for extra enhancement of metallic lithium stability with this type of coatings. Further chemical and spectroscopic analysis would be necessary to propose a more definite mechanism for the coating reaction.

A careful selection of coating agents and the optimization of a few simple coating parameters in the coating procedure can lead to the tailoring of desirable functional properties of protective coatings for metallic lithium electrodes, as reflected by the electrochemical performance recorded. In terms of cycle life, capacity relative to uncoated lithium, and EIS response before and after cycling, metallic lithium electrodes protected with coatings derived from $FpSiPh_3$ clearly outperform all other coatings tested in this study, and uncoated lithium itself. There are at least three possible factors involved in this enhancement. Without doubt, the physical barrier imposed by the coating between bare lithium and the electrolyte inhibits decomposition of the electrolyte by primary SEI formation, and leads to a more stable secondary SEI during cycling. We have strong evidence that coating thickness can be optimized by the combined factors of dip-coating time and less surface accessibility of the coating agent due to the bulky nature of the phenyl groups. Electron-rich phenyl groups might also offer enhanced conductance when compared to methyl-substituted silanes or to the redox-formed compounds of the primary SEI. However, a more

important aspect of the protection and cycle life enhancement conferred by the $FpSiPh_3$ derived coatings appears to be the stability of the secondary SEI formed electrochemically during cycling. Based on the promising performance demonstrated, other phenyl-substituted silanes with different co-substituents and leaving groups could provide interesting alternatives in the wet-chemical processing of protective coatings for metallic lithium electrodes.

4. Conclusions

We have investigated the electrochemical performance of metallic lithium electrodes protected by coatings derived from four different cyclopentadienyldicarbonyl iron (II) silanes (Fp-silanes). All the half cells made with the coated electrodes have shown enhanced cycle life when compared with uncoated lithium cycled under the same conditions and at similar cycling rates (1–2 C). Cycle life enhancements of up to 500% of that of uncoated lithium (60 cycles uncoated vs. > 300 cycles coated) were obtained. However, we observed a trade-off between cycle life and stable capacity. The best compromise was obtained for lithium electrodes dip-coated for 10 min with $FpSiPh_3$-derived coatings. We were able to identify a strong correlation between the chemical structure of the coating agent, the dip-coating time, the interphasial impedance, and cycle life performance. Cycle life enhancement seems to stem mainly from a higher stability of the secondary SEI formed during cycling in the coated electrodes. The promising performance obtained from these coatings suggests that other phenyl-substituted silanes could also be interesting for wet-chemistry processing of protective coatings for metallic lithium. Overall, our results imply that application-tailored protective coatings might, in the near future, enable the efficient use of metallic lithium electrodes in rechargeable batteries.

Acknowledgments

Support from the Batteries for Advanced Transportation Technologies (BATT) Program, Office of Vehicle Technologies Program, the U.S. Department of Energy, Office of Energy Efficiency and Renewable Energy, David Howell and Tien Duong, is gratefully acknowledged. SEM images were recorded using the equipment at the Electron Microscopy Center for Materials Research, Argonne National Laboratory; a US Department of Energy Office of Science Laboratory operated under Contract No. DE-AC02-06CH11357 by UChicago Argonne, LLC. S. N. would like to acknowledge the support of Gratz University of Technology through the FreChe Materie program.

References

[1] A. Kraytsberg, Y. Ein-Eli, J. Power Sources 196 (2011) 886–893.
[2] B. Dunn, H. Kamath, J.-M. Tarascon, Science 334 (2011) 928–935.
[3] S. Xiong, K. Xie, Y. Diao, X. Hong, Ionics 18 (2012) 867–872.
[4] P. Serras, V. Palomares, A. Goñi, P. Kubiak, T. Rojo, J. Power Sources 241 (2013) 56–60.
[5] M. Winter, J.O. Besenhard, M.E. Spahr, P. Novák, Adv. Mater. 10 (1998) 725–763.
[6] N. Munichandraiah, L.G. Scanlon, R.A. Marsh, J. Power Sources 72 (1998) 203–210.
[7] D. Aurbach, J. Power Sources 89 (2000) 206–218.
[8] C.M. López, J.T. Vaughey, D.W. Dees, J. Electrochem. Soc. 156 (2009) A726–A729.
[9] C.M. López, J.T. Vaughey, D.W. Dees, J. Electrochem. Soc. 159 (2012) A873–A886.
[10] J. Wen, Y. Yu, C. Chen, Mater. Express 2 (2012) 197–212.
[11] R.S. Thompson, D.J. Schroeder, C.M. López, S. Neuhold, J.T. Vaughey, Electrochem. Commun. 13 (2011) 1369–1372.
[12] S. Neuhold, D.J. Schroeder, J.T. Vaughey, J. Power Sources 206 (2012) 295–300.
[13] F. Marchioni, K. Star, E. Menke, T. Buffeteau, L. Servant, B. Dunn, F. Wudl, Langmuir 23 (2007) 11597–11602.
[14] M. Wu, Z. Wen, J. Jin, Y. Cui, Electrochim. Acta 103 (2013) 199–205.
[15] M. Ishikawa, S.I. Machino, M. Morita, Electrochemistry 67 (1999) 1200–1202.
[16] G.A. Umeda, E. Menke, M. Richard, K.L. Stamm, F. Wudl, B. Dunn, J. Mater. Chem. 21 (2011) 1593–1599.
[17] M.-Y. Chu, L. De Jonghe, S. Visco, in: Proceedings of the Annual Battery Conference on Applications and Advances, 1996, pp. 163–165.
[18] S.J. Visco, E. Nimon, B. Katz, M.Y. Chu, L.C. De Jonghe, in: AABC 2010-Advanced Automotive Battery Conference, 2010.
[19] B. Key, D.J. Schroeder, B.J. Ingram, J.T. Vaughey, Chem. Mater. 24 (2011) 287–293.
[20] S.M. Choi, I.S. Kang, Y.-K. Sun, J.-H. Song, S.-M. Chung, D.-W. Kim, J. Power Sources 244 (2013) 363–368.
[21] New Sci. 214 (2012) 27.
[22] T. Zhang, N. Imanishi, S. Hasegawa, A. Hirano, J. Xie, Y. Takeda, O. Yamamoto, N. Sammes, J. Electrochem. Soc. 155 (2008) A965–A969.
[23] H. Kitaura, H. Zhou, Energy Environ. Sci. 5 (2012) 9077–9084.
[24] P. Kichambare, S. Rodrigues, Energy Technol. 1 (2013) 209–211.
[25] W.J. van Ooij, D. Zhu, M. Stacy, A. Seth, T. Mugada, J. Gandhi, P. Puomi, Tsinghua Sci. Technol. 10 (2005) 639–664.
[26] C. Grogger, H. Fallmann, G. Fürpaß, H. Stüger, G. Kickelbick, J. Organomet. Chem. 665 (2003) 186–195.
[27] R.D. Theys, M.E. Dudley, M.M. Hossain, Coord. Chem. Rev. 253 (2009) 180–234.
[28] S. Neuhold, J. Albering, M. Flock, C. Grogger, ECS Trans. 19 (2009) 39–41.
[29] D.P. Abraham, M.M. Furczon, S.H. Kang, D.W. Dees, A.N. Jansen, J. Power Sources 180 (2008) 612–620.
[30] Y. Zhu, Y. Li, M. Bettge, D.P. Abraham, J. Electrochem. Soc. 159 (2012) A2109–A2117.

Glossary

Fp: cyclopentadienyldicarbonyl iron (II)
Fp_2: cyclopentadienyldicarbonyl iron (II) dimer
$ClSiR_3$: chlorosilane, R = H, Me, or Ph
H: hydrogen
Me: methyl group (CH_3)
Ph: phenyl group (C_6H_5)